Journal of Solid State Chemistry **156,** 339–348 (2001)
doi:10.1006/jssc.2000.9004, available online at http://www.idealibrary.com on IDEAL®

Phase Formation in $Cu_{3+1.5x}R_{4-x}(VO_4)_6$ (R = Fe and Cr) Systems: Crystal Structure of $Cu_{2.5}Fe_{4.333}(VO_4)_6$, $Cu_4Fe_{3.333}(VO_4)_6$, and $Cu_{4.05}Cr_{3.3}(VO_4)_6$

A. A. Belik, A. P. Malakho, K. V. Pokholok, and B. I. Lazoryak[1]

Department of Chemistry, Moscow State University, 119899 Moscow, Russia

Received June 14, 2000; in revised form September 27, 2000; accepted October 13, 2000; published online December 21, 2000

Phase formation in the $Cu_{3+1.5x}R_{4-x}(VO_4)_6$ (R = Fe and Cr) systems was studied at 670°C by powder X-ray diffraction. In the $Cu_{3+1.5x}Fe_{4-x}(VO_4)_6$ system there are two compounds having homogeneity ranges with formula $Cu_{3+1.5x}Fe_{4-x}(VO_4)_6$ ($0.667 \le x < 0.778$) and $Cu_{3+1.5x}Fe_{4-x}(VO_4)_6$ ($-0.333 \le x \le -0.167$) with structures of mineral lyonsite and mineral howardevansite (or $Fe_7(PO_4)_6$), respectively. The structures of $Cu_{2.5}Fe_{4.333}(VO_4)_6$ and $Cu_4Fe_{3.333}(VO_4)_6$ were refined by Rietveld method: space group $P\bar{1}$, $Z = 1$, $a = 6.6139(1)$ Å, $b = 8.0468(2)$ Å, $c = 9.7566(2)$ Å, $\alpha = 106.047(2)$, $\beta = 103.806(2)$, $\gamma = 102.157(2)$ for $Cu_{2.5}Fe_{4.333}(VO_4)_6$ and space group $Pnma$, $Z = 2$, $a = 4.91029(7)$ Å, $b = 10.2867(1)$ Å, $c = 17.2135(2)$ Å for $Cu_4Fe_{3.333}(VO_4)_6$. In the structure of $Cu_{2.5}Fe_{4.333}(VO_4)_6$ vacancies are localized in the octahedral Cu(1) sites. Specimens $Cu_{2.5}Fe_{4.333}(VO_4)_6$, $Cu_{2.75}Fe_{4.167}(VO_4)_6$, and $Cu_4Fe_{3.333}(VO_4)_6$ were characterized by Mossbauer spectroscopy. There are three components in Mossbauer spectra for the first two compounds. Iron cations in them occupy two octahedral sites and partially occupy a trigonal–bipyramidal site. In the $Cu_{3+1.5x}Cr_{4-x}(VO_4)_6$ system only one homogeneity range was found ($0.667 \le x \le 0.75$). The compound $Cu_{4.05}Cr_{3.3}(VO_4)_6$ was isolated and determined to be isotypic to lyonsite and some molybdates and tungstates. The crystal structure of the compound $Cu_{4.05}Cr_{3.3}(VO_4)_6$ was refined by Rietveld method (space group $Pnma$, $Z = 2$, $a = 4.89650(8)$ Å, $b = 10.2035(2)$ Å, $c = 17.1407(3)$ Å). The face-sharing octahedra $M(3)O_6$ form chains along the (100) direction and are partially occupied by Cu^{2+}. Copper cations locate on the faces of the edge-sharing prisms $M(1)O_6$ which also form chains along the (100) direction. The edge- and corner-sharing octahedra $M(2)O_6$ are occupied by Cu^{2+} and Cr^{3+} and constitute incomplete layers in the (001) plane. © 2001 Academic Press

Key Words: **vanadates; copper; iron; chromium; crystal structure; Rietveld method; Mossbauer spectroscopy.**

1. INTRODUCTION

New modifications of copper\iron vanadate and their single crystal structure solution have been described recently: orthorhombic (space group $Pnma$, $Z = 2$) mineral lyonsite, α-$Cu_3Fe_4(VO_4)_6$ (1) and triclinic (space group $P\bar{1}$, $Z = 1$) synthetic compound, β-$Cu_3Fe_4(VO_4)_6$ (2). The crystal structures of α- and β-$Cu_3Fe_4(VO_4)_6$ are distinguished significantly and cannot be derived one from another. β-$Cu_3Fe_4(VO_4)_6$ was obtained at 750°C by solid-state reaction from oxides or orthovanadates (2). The phase transition $\alpha \leftrightarrow \beta$ has not been studied yet. Parmer *et al.* (3) mentioned the existence of $Cu_3Fe(VO_4)_3$ and described the synthesis and structure refinement of $Cu_6Fe_{0.9}V_6O_{19}$. Wang *et al.* (4) reported about the synthesis and crystal structures of $Co_4Fe_{3.33}(VO_4)_6$ (isotypic with α-$Cu_3Fe_4(VO_4)_6$) and $Mn_3Fe_4(VO_4)_6$ (isotypic with β-$Cu_3Fe_4(VO_4)_6$).

Two triple vanadates, mineral howardevansite, $NaCuFe_2(VO_4)_3$ (5), and synthetic compound, $LiCuFe_2(VO_4)_3$ (6), which are isotypic with β-$Cu_3Fe_4(VO_4)_6$, were reported. $NaCuFe_2(VO_4)_3$ and $LiCuFe_2(VO_4)_3$ are formed during substitution $Cu^{2+} \rightarrow 2M^+$ in β-$Cu_3Fe_4(VO_4)_6$. They are of interest because some alkali cations are located in the large cavity $M(5)O_{10}$, which is empty in the structure of β-$Cu_3Fe_4(VO_4)_6$. Alkali cations in the $M(5)O_{10}$ cavity are strongly displaced from the special position in the center of symmetry $(0, 0, \frac{1}{2})$ to a half-occupied general position. β-$Cu_3Fe_4(VO_4)_6$ is isotypic with some orthophosphates, $Me_3^{2+}R_4^{3+}(PO_4)_6$ and $Me_7H_x(PO_4)_6$ (7, and Refs. therein), and molybdates, $Ag_2Zn_2(MoO_4)_3$ (8) and $NaMg_{2.5}(MoO_4)_3$ (9), with all of them having the $Fe_7(PO_4)_6$ structure type (10). The number of cations per unit cell in this structure type changes from 7 to 8. α-$Cu_3Fe_4(VO_4)_6$ is isotypic with some molybdates, $Li_2Fe_2(MoO_4)_3$ (11), $Li_3R(MoO_4)_3$ (R = Fe (11), Al, Ga, Cr, Sc, In (12)), $Li_2Me_2(MoO_4)_3$, $Na_{2-2x}Me_{2+x}(MoO_4)_3$ (Me = Mg, Zn, Co, and Cu (12, 13)), and others (vide infra, Table 6) and tungstate $Li_2Mg_2(WO_4)_3$ (12). Some molibdates, $Na_2Me_2(MoO_4)_3$ (Me = Cu, Zn) and $Li_2Cu_2(MoO_4)_3$ (14) have high ionic conductivity, for example ca. 5.8×10^{-3} ohm^{-1} cm^{-1} at 400°C for $Li_2Cu_2(MoO_4)_3$ (14). The structure of α-$Cu_3Fe_4(VO_4)_6$ (1) has one partially occupied position that gives possibilities for nonstoichiometry as

[1]To whom correspondence should be addressed. Fax: (095) 938 24 57. E-mail: lazoryak@tech.chem.msu.ru.

0022-4596/01 $35.00

in $Co_4Fe_{3.33}(VO_4)_6$ (4). The full occupation of this position (16 cations per unit cell) is realized in some molybdates. To our knowledge, other vanadates with α- and β-$Cu_3Fe_4(VO_4)_6$ structures were not reported. The above-mentioned facts indicate that the cation sublattice of the structure types in which α- and β-$Cu_3Fe_4(VO_4)_6$ are crystallized may contain different number of cations and suggest the existence of homogeneity ranges. Homogeneity range for the above-mentioned vanadates have not been studied yet.

In this work, we report about the phase formation of double vanadates $Me_{3+1.5x}R_{4-x}(VO_4)_6$ (Me = Cu, R = Fe and Cr) in the range $-0.5 \le x \le 2$ and the crystal structures of $Cu_{2.5}Fe_{3.333}(VO_4)_6$, $Cu_4Fe_{3.333}(VO_4)_6$, and $Cu_{4.05}Cr_{3.3}(VO_4)_6$ by powder X-ray diffraction.

2. EXPERIMENTAL

Synthesis

Specimens were synthesized from stoichiometric mixtures of CuO, Cr_2O_3, Fe_2O_3, and V_2O_5 at different temperatures under air in Pt crucibles. After annealing specimens were quenched in air. All specimens were black or dark-brown.

X-ray Diffraction Data Collection

X-ray diffraction (XRD) patterns for phase analysis were recorded at room temperature on a SIEMENS D500 powder diffractometer equipped with a SiO_2 incident-beam monochromator ($CuK\alpha_1$ radiation at 30 kV and 30 mA, Ni-filter, $\lambda = 1.5406$ Å) and a Braun position-sensitive detector. Data were collected between $2\Theta = 8$–60° with a step interval of 0.02°. Effective counting time per step was 3–10 min.

X-ray pattern processing and quantitative phase analysis were performed by full-profile fitting using the Rietveld refinement program RIETAN-97 (15). During the Rietveld processing for quantitative phase analysis only scale factors and cell parameters for α-$Cu_3Fe_4(VO_4)_6$ (1), β-$Cu_3Fe_4(VO_4)_6$ (2), $CrVO_4$ (16), Cr_2O_3 (17), α-$Cu_2V_2O_7$ (18), $CuCr_2O_4$ (19), and $Cu_{4.05}Cr_{3.30}(VO_4)_6$ were refined. In some cases the quantitative phase analysis was performed using corundum as the internal standard.

For structural refinements X-ray diffraction patterns were collected on the same diffractometer. Counting conditions are given in Table 1. Effective counting time per step was ca. 30 min. The scattering factors for Cu^{2+}, Cr^{3+}, Fe^{3+}, V, and

TABLE 1
Important Refined Parameters and Counting Conditions for β-$Cu_{2.5}Fe_{4.333}(VO_4)_6$, α-$Cu_{4.05}Cr_{3.3}(VO_4)_6$, and α-$Cu_4Fe_{3.333}(VO_4)_6$

	β-$Cu_{2.5}Fe_{4.333}(VO_4)_6$	α-$Cu_{4.05}Cr_{3.3}(VO_4)_6$	α-$Cu_4Fe_{3.333}(VO_4)_6$
Space group	*P*-1 (No. 2)	*Pnma* (No. 62)	*Pnma* (No. 62)
Z	1	2	2
2Θ Range (°)	8–105	8–105	8–120
Scan step	0.02	0.02	0.02
I_{max}/I_{back}[a](counts)	45599/13240	34205/2505	42550/12095
Lattice constants			
a (Å)	6.6139(1)	4.89650(8)	4.91029(7)
b (Å)	8.0468(2)	10.2035(2)	10.2867(1)
c (Å)	9.7566(2)	17.1407(3)	17.2135(2)
α	106.047(2)	90	90
β	103.806(2)	90	90
γ	102.157(2)	90	90
V (Å^3)	462.8	856.4	869.5
No. of Bragg reflections	1059	523	688
Variables			
Structural/Others	73/27	43/18	43/23
Texture parameter[b]	0.880(2)	0.930(2)	—
Texture vector	(010)	(001)	
Reliable factors[c]			
R_{WP}; R_P	0.93; 0.74	4.81; 3.61	0.99; 0.78
R_I; R_F	2.84; 2.13	6.51; 4.39	3.13; 2.13
S	1.09	2.23	1.09
D-W d	1.73	0.45	1.63

[a] I_{back} is background intensity near the maximum peak.
[b] Texture was modeled by March-Dollase function.
[c] Defined as in (15).

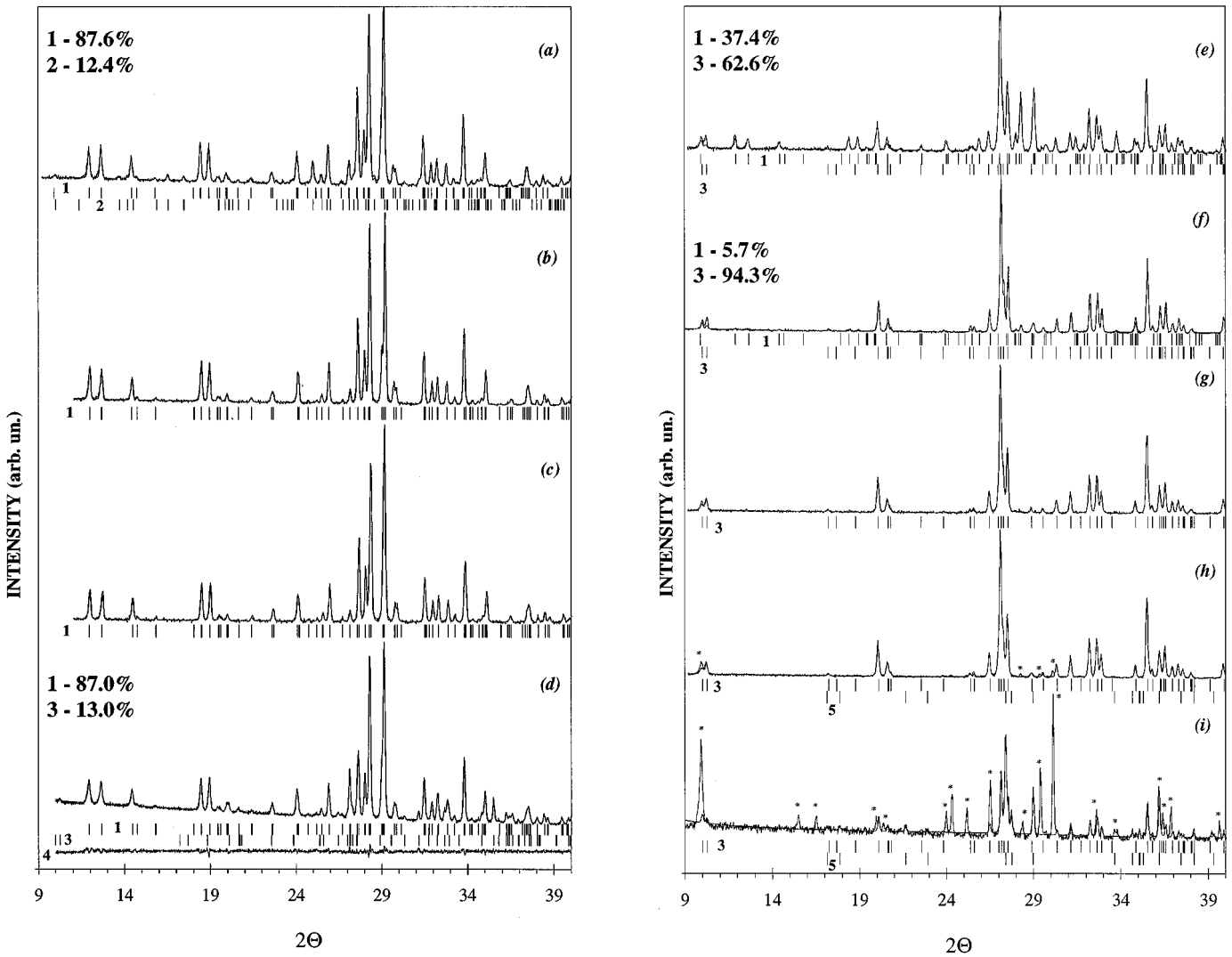

FIG. 1. X-ray diffraction patterns of $Cu_{3+1.5x}Fe_{4-x}(VO_4)_6$ with $x = -0.5$ (*a*) $-\frac{1}{3}$ (*b*) $-\frac{1}{6}$ (*c*) 0.0 (*d*) $\frac{1}{3}$ (*e*) 0.6 (*f*) $\frac{2}{3}$ (*g*) $\frac{7}{9}$ (*h*) and 2 (*i*) after the Rietveld processing of XRD data. Bragg reflections for β-modification (1), $FeVO_4$ (2), α-modification (3), and α-$Cu_2V_2O_7$ (5) are shown. Reflections of the unidentified phase are marked by (*). 4, Difference X-ray pattern. Experimental weight fractions of phases (from Rietveld processing of XRD data) are given.

O^- were used. TCH modified pseudo-Voigt function (15) was used for profile fitting and 11th (or 5th)-order polynom was used for background fitting. Peak asymmetry was corrected according the procedure of Howard. Standard deviations were estimated by the conventional method.

Mossbauer Spectroscopy

Iron-57 Mossbauer spectra were recorded at room temperature using a constant acceleration Mossbauer spectrometer coupled with a 1024 multichannel analyzer and a $^{57}Co/Rh$ source kept at RT. All isomer shift values (δ) given hereafter are referred to α-iron. Experimental data were resolved into symmetric quadrupole doublets with Lorentzian lineshapes using an iterative least-square fit program.

3. RESULTS AND DISCUSSION

Study of $Cu_{3+1.5x}Fe_{4-x}(VO_4)_6$ ($-0.5 \le x \le 2$)

First, we tried to synthesize the compound β-$Cu_3Fe_4(VO_4)_6$ using conditions (750°C, 50 h, slow cooling) given in (2). XRD showed that the specimen consisted of a mixture of two phases isotypic with β- and α-$Cu_3Fe_4(VO_4)_6$ (hereafter, β- and α-modifications). The Rietveld processing of X-ray pattern without the refinement of atomic coordinates of β-modification (2) and α-modification (1) gave a very good agreement between the observed and calculated patterns ($R_{WP} = 2.30$, $R_p = 1.75$, $S = 1.52$;

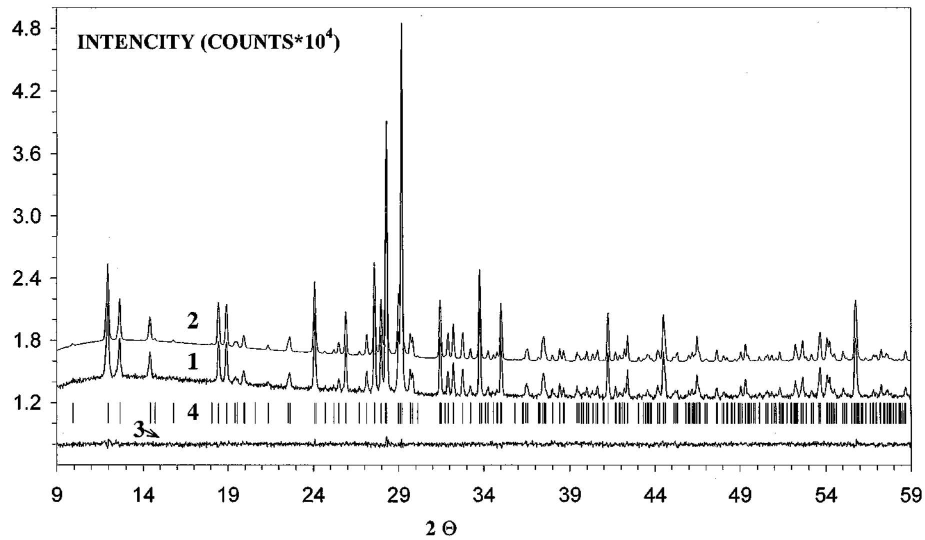

FIG. 2. Portion of the Rietveld refinement profiles for β-$Cu_{2.5}Fe_{4.333}(VO_4)_6$. 1, observed, 2, calculated; and 3, difference X-ray powder diffraction patterns; 4, Bragg reflections. The calculated pattern is shifted to 3500 counts from the observed pattern.

$R_I = 6.43$, $R_F = 5.10$ for β-modification, and $R_I = 6.59$, $R_F = 5.17$ for α-modification). The obtained weight portion of α-modification was 13.6 wt%. A slow cooling (ca. 10°/h) of this sample and a long treatment (50 h) at 600 and 500°C did not change the phase composition.

Then we tried to synthesize $Cu_3Fe_4(VO_4)_6$ at lower temperatures. The synthesis at 670°C gave a mixture of β- and α- (13.5 wt%) modifications. The following treatment of this specimen at 800°C (2 h) gave the same phase composition, i.e., a mixture of β- and α- (13.0 wt%) modifications. Annealing at 900°C (2 h) resulted in the decomposition of the specimen. The powder consisted of α-modification, Fe_2O_3, and an unidentified phase (three strongest lines: $d = 3.035$, 7.30, 3.606 Å).

The synthesis of the $Cu_3Fe_4(VO_4)_6$ compound at 500°C (for 2 weeks) gave a mixture of β- and α- (traces) modifications, Fe_2O_3, and CuV_2O_6 (JCPDS Card 45-1054). Anneal-

TABLE 2
Atomic Positional and Isotropic Displacement Parameters for β-$Cu_{2.5}Fe_{4.333}(VO_4)_6$

Atom	x	y	z	B_{iso}
Cu(1)	0	0.5	0.5	0.5(2)
Cu(2)	0.7258(8)	0.7147(7)	0.2115(7)	2.2(2)
Fe(1)	0.381(1)	0.9477(8)	0.6078(8)	1.8(2)
Fe(2)	0.040(1)	0.2071(6)	0.0124(7)	1.0(2)
V(1)	0.892(1)	0.9009(7)	0.6639(8)	1.4(2)
V(2)	0.224(1)	0.6585(7)	0.2681(7)	1.4(2)
V(3)	0.592(1)	0.2709(8)	0.1232(8)	1.9(2)
O(1)	0.072(3)	0.061(2)	0.137(2)	1.0(6)
O(2)	0.555(3)	0.146(2)	0.228(2)	2.2(7)
O(3)	0.180(4)	0.430(2)	0.182(2)	1.7(6)
O(4)	0.979(3)	0.276(2)	0.826(2)	0.0(5)
O(5)	0.231(3)	0.778(3)	0.956(3)	0.7(6)
O(6)	0.859(3)	0.987(2)	0.353(2)	0.0(5)
O(7)	0.527(3)	0.227(2)	0.737(2)	0.0(5)
O(8)	0.333(4)	0.227(2)	0.990(3)	1.3(6)
O(9)	0.338(3)	0.046(3)	0.422(2)	1.3(6)
O(10)	0.202(3)	0.683(2)	0.465(2)	2.4(6)
O(11)	0.693(3)	0.493(2)	0.236(2)	1.4(6)
O(12)	0.125(3)	0.302(2)	0.414(2)	0.8(6)

Note. Occupancy of the Cu(1) site is 0.833; occupancy of the Cu(2) site is $0.833Cu^{2+} + 0.167Fe^{3+}$; occupancy of other sites is 1.

TABLE 3
Parameters of Mossbauer Spectra for β-$Cu_{2.5}Fe_{4.333}(VO_4)_6$, β-$Cu_{2.75}Cr_{4.167}(VO_4)_6$, and α-$Cu_4Fe_{3.333}(VO_4)_6$ at Room Temperature

Compound	δ^a (mm/s)	$\Delta E_Q{}^b$ (mm/s)	Γ^c (mm/s)	S^d (%)
β-$Cu_{2.5}Fe_{4.333}(VO_4)_6$	0.43(1)	0.95(1)	0.31(1)	42(2)
	0.41(1)	0.64(1)	0.31(1)	47(2)
	0.26(2)	1.09(2)	0.24(2)	11(2)
	0.44(1)	1.00(1)	0.30(1)	47(2)
β-$Cu_{2.75}Fe_{4.167}(VO_4)_6$	0.42(1)	0.69(1)	0.31(1)	43(2)
	0.28(2)	1.14(2)	0.25(2)	10(2)
	0.40(2)	1.01(2)	0.29(2)	49(3)
β-$Cu_3Fe_4(VO_4)_6$	0.38(2)	0.69(2)	0.31(2)	43(3)
(2)	0.25(2)	1.14(2)	0.25(2)	8(3)
α-$Cu_4Fe_{3.333}(VO_4)_6$	0.48(1)	0.45(2)	0.35(1)	57(2)
	0.49(1)	0.74(2)	0.35(1)	43(2)

[a] Chemical shift.
[b] Quadrupole splitting.
[c] Full width at half maximum.
[d] Area.

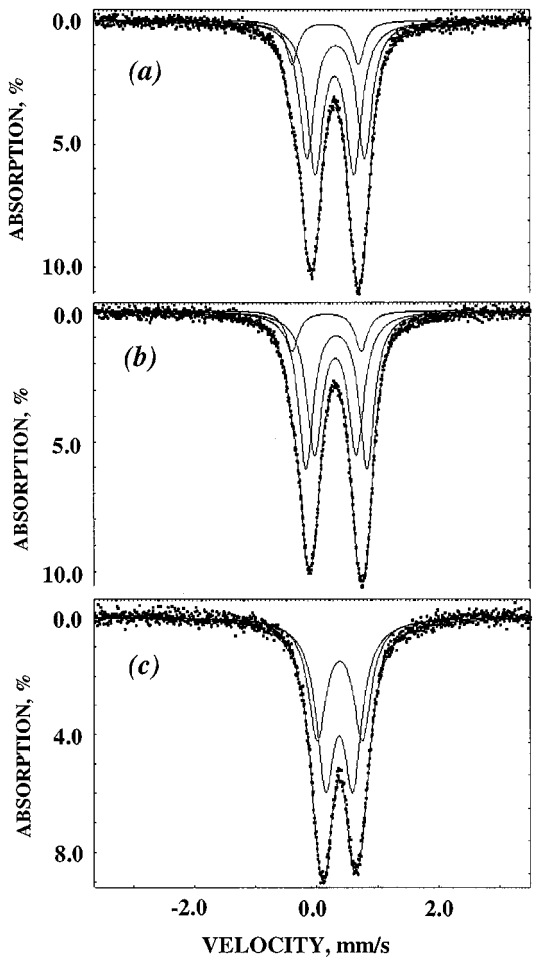

FIG. 3. Mossbauer spectra of specimens (*a*) β-$Cu_{2.5}Fe_{4.333}(VO_4)_6$, (*b*) β-$Cu_{2.75}Fe_{4.167}(VO_4)_6$, and (*c*) α-$Cu_4Fe_{3.333}(VO_4)_6$ at room temperature.

ing of this specimen at 600°C (50 h) gave a mixture of β- and α- (13.0 wt%) modifications. Thus, attempts to synthesize pure β-$Cu_3Fe_4(VO_4)_6$ and avoid the formation of α-modification were not successful. The obtained results may indicate that the composition of β- and α-$Cu_3Fe_4(VO_4)_6$ deviates from stoichiometric that makes it necessary to study the phase formation in this system. Note that single crystals of $Co_4Fe_{3.33}(VO_4)_6$ were obtained from the specimen with the total composition of $Co_3Fe_4(VO_4)_6$ (4).

We have investigated the phase formation in the $Cu_{3+1.5x}Fe_{4-x}(VO_4)_6$ system at $-0.5 \le x \le 2$. The specimens were annealed at 670°C (100 h) followed by quenching in air. The results are shown in Fig. 1. The specimen with $x = -0.5$ was a mixture of $FeVO_4$ and β-modification, while the specimens with $x = -\frac{1}{3}$ and $-\frac{1}{6}$ were single-phased (Fig. 1). Appearance of $FeVO_4$ at $x = -0.5$ suggests that no new compounds are formed at $-2 \le x \le -0.5$. The specimens with $x = 0$, $\frac{1}{3}$, and 0.6 consisted of a mixture of β- and α-modifications. The specimens with $x = \frac{2}{3}$ had only α-modification, while the specimens with $x = \frac{7}{9}$, 1, 1.5, and 2 had α-modification, α-$Cu_2V_2O_7$, and an unidentified phase (three strongest lines: d = 2.966, 8.91, 3.038 Å) (Fig. 1*i*). Note that the specimens with $x = \frac{7}{9}$ had traces of α-$Cu_2V_2O_7$ and an unidentified phase.

Our results indicate that the reported two modifications of $Cu_3Fe_4(VO_4)_6$ are indeed two different compounds having homogeneity range with the composition $Cu_{3+1.5x}Fe_{4-x}(VO_4)_6$ ($0.667 \le x < 0.778$) for α-modification and $Cu_{3+1.5x}Fe_{4-x}(VO_4)_6$ ($-0.333 \le x \le -0.167$) for β-modification. (Hereafter, we use the labels β- and α- in order to clarify the structure type in which compounds are crystallized). Thus, the $Fe_7(PO_4)_6$ structure type can contain

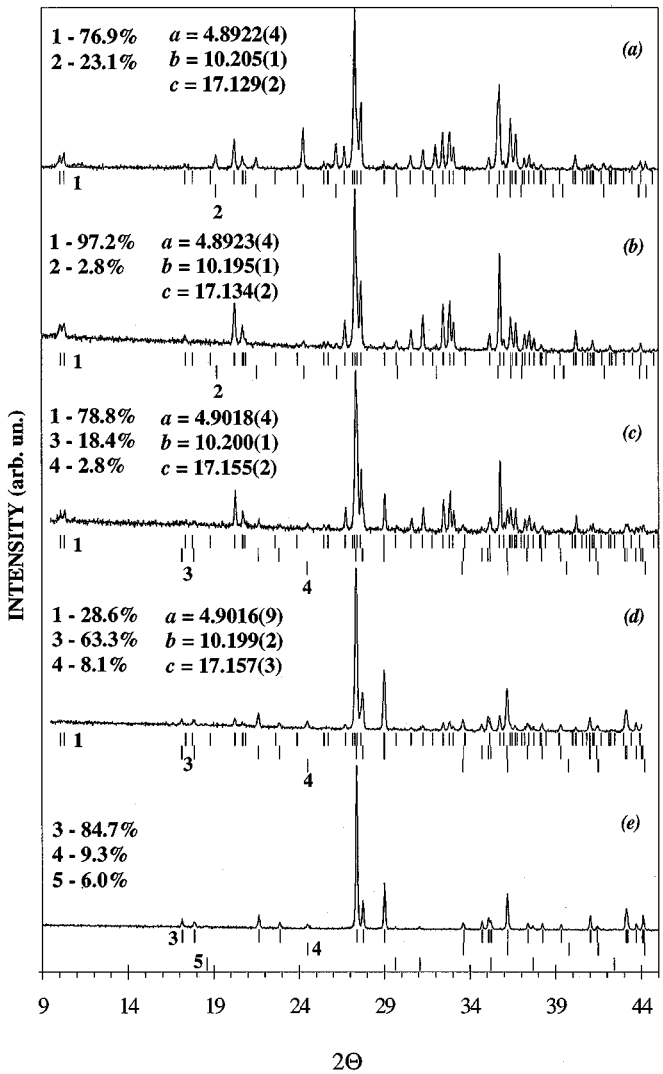

FIG. 4. X-ray diffraction patterns of $Cu_{3+1.5x}Cr_{4-x}(VO_4)_6$ with x = 0.0 (a), 0.6 (b), 1.0 (c), 1.6 (d), and 2.0 (e) after the Rietveld processing of XRD data. Bragg reflections for α-modification (1), $CrVO_4$ (2), α-$Cu_2V_2O_7$ (3), Cr_2O_3 (4), and $CuCr_2O_4$ (5) are shown. Experimental weight fractions of phases (from Rietveld processing of XRD data) and unit cell parameters (Å) for α-modification are given.

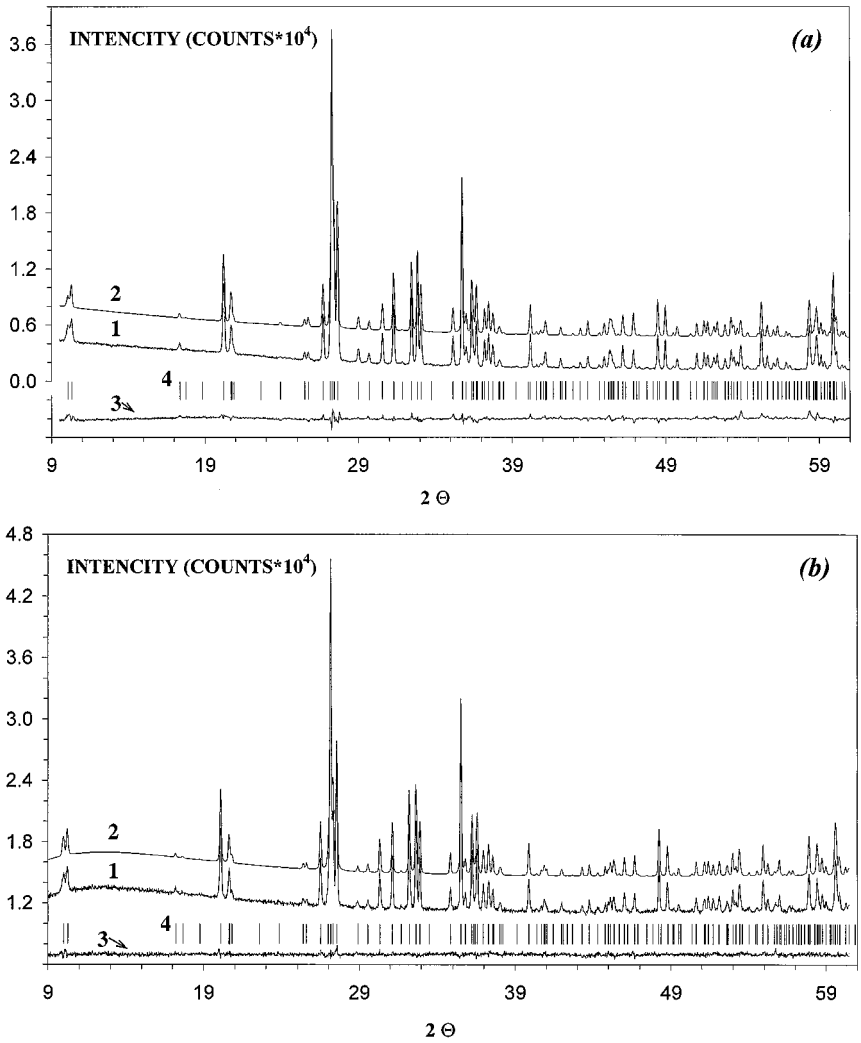

FIG. 5. Portion of the Rietveld refinement profiles for (*a*) α-$Cu_{4.05}Cr_{3.3}(VO_4)_6$ and (*b*) α-$Cu_4Fe_{3.333}(VO_4)_6$. 1, Observed; 2, calculated; and 3, difference X-ray powder diffraction patterns; 4, Bragg reflections. The calculated patterns are shifted to 3500 counts from the observed patterns.

fewer than seven cations per unit cell. Structure refinement of β-modification in the specimen with total composition $Cu_3Fe_4(VO_4)_6$ gave the following site occupancies: $n(Cu(1)) = 0.95(1)$ with $B_{iso} = 2.5$, $n(Cu(2)) = 0.99(1)$ with $B_{iso} = 2.5$, $n(Fe(1)) = 1.02(1)$ with $B_{iso} = 1.0$, and $n(Fe(2)) = 1.00(1)$ with $B_{iso} = 1.0$ and the following R factors: $R_{WP} = 2.01$, $R_p = 1.59$, $S = 1.34$; $R_I = 5.71$, $R_F = 4.56$ for β-modification and $R_I = 6.05$, $R_F = 4.55$ for α-modification. A portion of the Rietveld refinement profiles for $Cu_3Fe_4(VO_4)_6$ is shown in Fig. 1*d*. The values of site occupancies may suggest that vacancies are localised in the Cu(1) site. The refinement of the crystal structure of β-$Cu_{2.5}Fe_{4.333}(VO_4)_6$ has also confirmed that vacancies are mainly localized in the Cu(1) sites: $n(Cu(1)) = 0.84(1)$ with $B_{iso} = 0.5$, $n(Cu(2)) = 0.99(1)$ with $B_{iso} = 2.5$, $n(Fe(1)) = 1.02(1)$ with $B_{iso} = 1.0$, and $n(Fe(2)) = 1.00(1)$ with $B_{iso} = 1.0$. As was expected, the occupancy of the Cu(1) sites for β-$Cu_{2.5}Fe_{4.333}(VO_4)_6$ is less than for β-modification in the $Cu_3Fe_4(VO_4)_6$ specimen. The important refinement conditions, refined lattice parameters, and R factors are presented in Table 1. The final observed, calculated, and difference Rietveld profiles are shown in Fig. 2. The refined atomic coordinates, thermal parameters for β-$Cu_{2.5}Fe_{4.333}(VO_4)_6$ are listed in Table 2. $Mn_3Fe_4(VO_4)_6$ was reported to be stoichiometric (4), but the value of the obtained thermal parameter for the Mn(1) site ($B_{iso} = 2.1$) in comparison to other thermal parameters ($B_{iso}(Mn(2)) = 0.5$, $B_{iso}(Fe(1)) = 0.4$, and $B_{iso}(Fe(2)) = 0.4$) (4) may also indicate the slight deviation in stoichiometry as we have found for β-$Cu_{3+1.5x}Fe_{4-x}(VO_4)_6$ ($-0.333 \leq x \leq -0.167$).

Mossbauer spectra of β-$Cu_{2.5}Fe_{3.333}(VO_4)_6$, β-$Cu_{2.75}Fe_{4.167}(VO_4)_6$, and α-$Cu_4Fe_{3.333}(VO_4)_6$ are shown in Fig. 3.

Table 3 gives the parameters of these spectra. The spectra of β-$Cu_{2.5}Fe_{3.333}(VO_4)_6$ and β-$Cu_{2.75}Fe_{4.167}(VO_4)_6$ are very close to the spectrum of β-$Cu_3Fe_4(VO_4)_6$ given in (2) and also have the third component with the smaller isomer shift value ($\delta = 0.26$–0.28 mm/s). This isomer shift suggests the fivefold coordination for Fe^{3+} according to Menil (20) ($0.22 \le \delta \le 0.34$ mm/s for CN = 5, $0.30 \le \delta \le 0.50$ mm/s for CN = 6). Lafontaine *et al.* (2) explained the appearance of this component in the spectrum by the cation inversion between the $Cu(2)O_5$ and $Fe(1)O_6$ and(or) $Fe(2)O_6$ sites. However, deviation in the composition of β-$Cu_{3+1.5x}Fe_{4-x}(VO_4)_6$ ($-0.333 \le x \le -0.167$) results in the excess of iron cations which must occupy the $Cu(1)O_{[4+2]}$ and(or) $Cu(2)O_5$ sites and give the third component in Mossbauer spectrum. Note that cation inversion between the $Cu(2)O_5$ and $Fe(1)O_6$ and/or $Fe(2)O_6$ sites must take place as the expected area (7.7 and 4.0%) is less than the observed area (11 and 10%) for the third component in Mossbauer spectra of β-$Cu_{2.5}Fe_{3.333}(VO_4)_6$ and β-$Cu_{2.75}Fe_{4.167}(VO_4)_6$, respectively. The spectrum of α-$Cu_4Fe_{3.333}(VO_4)_6$ was fitted as two doublets. The isomer shifts for α-$Cu_4Fe_{3.333}(VO_4)_6$ are greater while quadrupole splitting is less than for β-$Cu_{2.5}Fe_{3.333}(VO_4)_6$ and β-$Cu_{2.75}Fe_{4.167}(VO_4)_6$.

TABLE 4
Atomic Positional and Isotropic Displacement Parameters for α-$Cu_{4.05}Cr_{3.3}(VO_4)_6$ (I) and α-$Cu_4Fe_{3.333}(VO_4)_6$ (II)

Atom		x	y	z	B_{iso}
$M(1)$	I	0.2071(8)	0.25	0.8233(2)	1.23(8)
	II	0.207(1)	0.25	0.8219(2)	1.1(1)
$M(2)$	I	0.2445(5)	0.4279(2)	0.9732(1)	0.10(6)
	II	0.2450(6)	0.4239(2)	0.9722(1)	0.35(7)
$M(3)$	II	0.9015(8)	0.75	0.7485(2)	1.0(1)
	II	0.909(1)	0.75	0.7484(3)	2.4(2)
V(1)	II	−0.2215(9)	0.25	0.0561(2)	0.95(9)
	II	−0.230(1)	0.25	0.0576(2)	0.9(1)
V(2)	I	0.7156(6)	0.4726(2)	0.8443(1)	0.78(7)
	II	0.7235(9)	0.4719(2)	0.8443(1)	0.93(9)
O(1)	I	0.653(2)	0.6207(7)	0.7933(4)	1.5(2)
	II	0.664(2)	0.6173(7)	0.7946(5)	1.7(3)
O(2)	I	0.420(2)	0.3889(8)	0.8726(4)	1.0
	II	0.427(2)	0.3868(9)	0.8711(5)	0.0(3)
O(3)	I	0.045(2)	0.25	0.9961(6)	0.7(3)
	II	0.057(3)	0.25	0.9951(7)	0.1(4)
O(4)	I	0.551(2)	0.3889(8)	0.0312(5)	1.9(3)
	II	0.563(2)	0.3862(9)	0.0313(6)	2.0(3)
O(5)	I	0.923(1)	0.5014(8)	0.9308(4)	0.7(2)
	II	0.922(2)	0.503(1)	0.9287(6)	1.8(3)
O(6)	I	0.652(3)	0.75	0.6514(6)	0.9(3)
	II	0.653(3)	0.75	0.6554(6)	0.2(4)
O(7)	I	−0.079(2)	0.3733(7)	0.7904(4)	1.2(2)
	II	−0.075(2)	0.3741(8)	0.7927(5)	1.1(3)

Note. Occupancies of the $M(1)$–$M(3)$ sites are given in Table 6.

TABLE 5
Bond Distances (Å) and Angles (°) for Tetrahedra VO_4^{3-} in $Cu_{4.05}Cr_{3.3}(VO_4)_6$

Bonds and angles		Bonds and angles	
$M(1)$–O(2)*2	1.952(9)	V(1)–O(3)	1.66(1)
–O(7)*2	1.966(8)	–O(4)*2	1.852(9)
$\langle M(1)$–O$\rangle$	1.959	–O(6)	1.67(1)
$M(1)$–O′(7)*2	2.545(8)	$\langle$V(1)–O$\rangle$	1.759
$M(2)$–O(2)	1.967(8)	O(3)–V(1)–O(4)	109.2(4)
–O(3)	2.097(6)	–O′(4)	109.2(4)
–O(4)	1.845(8)	–O(6)	116.5(6)
–O′(4)	2.122(8)	O(4)–V(1)–O′(4)	99.8(5)
–O(5)	1.889(7)	–O(6)	110.4(4)
–O′(5)	1.975(7)	O′(4)–V(1)–O(6)	110.4(4)
$\langle M(2)$–O$\rangle$	1.983	$\langle$O–V(1)–O$\rangle$	109.3
$M(3)$–O(1)*2	1.941(8)	V(2)–O(1)	1.773(7)
–O′(1)*2	1.953(8)	–O(2)	1.750(9)
–O(6)	2.06(1)	–O(5)	1.821(7)
–O′(6)	2.11(1)	–O(7)	1.700(8)
$\langle M(3)$–O$\rangle$	1.993	$\langle$V(2)–O$\rangle$	1.761
O(1)–V(2)–O(2)	114.2(5)	O(2)–V(2)–O(5)	108.3(4)
–O(5)	111.2(4)	–O(7)	10.4(4)
–O(7)	110.0(4)	O(5)–V(2)–O(7)	102.1(4)
		$\langle$O–V(2)–O$\rangle$	109.4

The Study of $Cu_{3+1.5x}Cr_{4-x}(VO_4)_6$ ($0 \le x \le 2$)

Synthesis of the specimen with the composition $Cu_3Cr_4(VO_4)_6$ at 600°C for 100 h gave a mixture of a phase isotypic to lyonsite (hereafter, α-modification) and $CrVO_4$ (23.0 wt%). The increasing of the treatment temperature up to 670°C (100 h) did not change significantly the phase composition ($CrVO_4$, 23.1 wt%). Heating at 750°C (50 h) resulted in the partial decomposition with a mixture of α-modification, Cr_2O_3, β-$Cu_2V_2O_7$ (JCPDS Card 73-1032), and an unidentified phase been obtained. Heating at 800°C (50 h) resulted in melting of the specimen which consisted of a mixture of Cr_2O_3, β-$Cu_2V_2O_7$, and the same unidentified phase (three strongest lines: $d = 3.396$, 2.714, 7.35 Å). The presence of $CrVO_4$ in the specimen with the composition $Cu_3Cr_4(VO_4)_6$ obtained below 670°C suggests that the composition is changed according to the scheme:

$$(1 + 0.5x)Cu_3Cr_4(VO_4)_6 \rightarrow 3xCrVO_4 + Cu_{3+1.5x}Cr_{4-x}(VO_4)_6.$$

The appearance of $CrVO_4$ suggests that no new compounds are formed in the $Cu_{3+1.5x}Cr_{4-x}(VO_4)_6$ system at $x < 0$. Phase formations in the $Cu_{3+1.5x}Cr_{4-x}(VO_4)_6$ system for $0 \le x \le 2$ were studied. The specimens were annealed at 670°C (100 h) followed by quenching in air. The specimens with $0 \le x \le 0.6$ consisted of mixtures of α-modification and $CrVO_4$ (Figs. 4a and 4b). The specimens with $0.8 \le x < 2.0$ consisted of mixtures of α-modification,

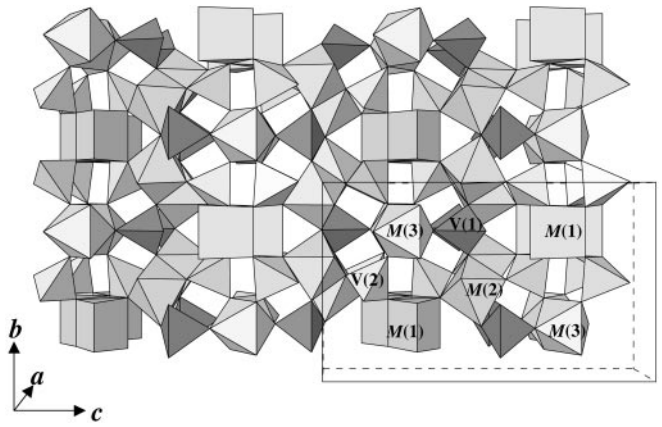

FIG. 6. The retrospective view along the (100) direction of crystal structure of α-$Cu_{4.05}Cr_{3.3}(VO_4)_6$.

Cr_2O_3, and α-$Cu_2V_2O_7$ (Figs. 4c and 4d). The specimens with $x = \frac{2}{3}$, 0.7, and 0.75 were single-phased. Unit cell parameters for α-modification were very close to each other in different specimens with $0 \le x < 2$. It indicates that the range of solid solutions in $Cu_{3+1.5x}Cr_{4-x}(VO_4)_6$ is narrow with $\frac{2}{3} \le x \le 0.75$.

Structure Refinement of α-$Cu_{4.05}Cr_{3.3}(VO_4)_6$ and α-$Cu_4Fe_{3.333}(VO_4)_6$

Refinement of the crystal structure of α-$Cu_{4.05}Cr_{3.30}(VO_4)_6$ was initiated in space group *Pnma* (No. 62) using initial structure model with atomic coordinates from mineral lyonsite (1). First, all the cation sites $M(1)$–$M(3)$ were filled by Cu^{2+} with occupancies equal to 1. Full occupation of these sites should lead to 16 cations per unit cell, while α-$Cu_{4.05}Cr_{3.3}(VO_4)_6$ has 14.7 cations per unit cell. After several cycles of refinement the following thermal parameters were obtained: $B_{iso} = 0.1(1)$ for $M(1)$, $B_{iso} = 0.9(1)$ for $M(2)$, and $B_{iso} = 6.7(2)$ for $M(3)$. The values of thermal parameters suggested that vacancies were localized in the $M(3)$ sites. As scattering factors of copper and chromium are close to each other, it was possible to examine boundary cation distributions. When chromium cations were placed into the $M(1)$ and(or) $M(3)$ sites the negative thermal parameters were obtained for these sites. The following cation distributions, $1Cu^{2+} - M(1)$, $0.175Cu^{2+} + 0.825Cr^{3+} - M(2)$, and $0.675Cu^{2+} + 0.325\square - M(3)$ gave reasonable thermal parameters for all sites. This cation distribution was used during refinement of the crystal structure. The same structure refinement strategy was used for the refinement of α-$Cu_4Fe_{3.333}(VO_4)_6$. The important refinement conditions, refined lattice parameters, and R factors are presented in Table 1. The final observed, calculated, and difference Rietveld profiles are shown in Fig. 5. The refined atomic coordinates, thermal parameters, and interatomic distances are listed in Tables 4 and 5.

Description of the Structure and Structural Relationships

Figure 6 gives the projection of the structure of α-$Cu_{4.05}Cr_{3.3}(VO_4)_6$ along the (100) direction. The structure consists of three types of cation polyhedra which form chains along the (100) direction. $M(3)O_6$ octahedra are face-shared (Fig. 7b) and are not linked to either cation polyhedra $M(1)O_6$ or $M(2)O_6$. The arrangement of VO_4^{3-} tetrahedra around the $M(3)O_6$ chains and the $M(3)O_6$ chains actually have trigonal symmetry. $M(2)O_6$ octahedra form zig-zag chains. They are linked with one another by edges O(3)–O(3) and O(4)–O(4) (Fig. 7a). The $M(2)O_6$ chains are linked with one another by common oxygens O(2) forming sheets perpendicular to the c axis (Fig. 7a). $M(1)O_6$ trigonal prisms form zig-zag single chains by sharing edges (Fig. 7c). The $M(1)O_6$ chains are linked with $M(2)O_6$ octahedra by corners and provide the connection between layers formed by $M(2)O_6$ octahedra.

The number of cations per unit cell in this structure type can be changed from 12 to 16. Some molybdates are not stoichiometric compounds and have a region of homogen-

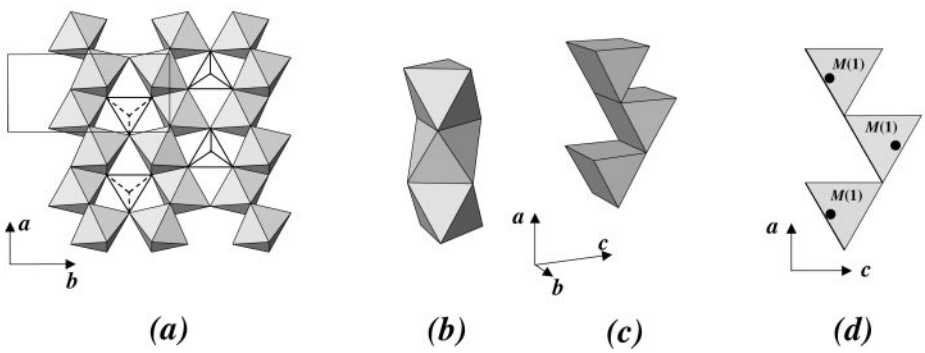

FIG. 7. The linkage of polyhedra in the structure of α-$Cu_{4.05}Cr_{3.3}(VO_4)_6$: (a) the layer of edge- and corner-sharing $M(2)O_6$ octahedra; (b) the chains of face-sharing $M(3)O_6$ octahedra, and (c) edge-sharing $M(1)O_6$ trigonal prisms; (d) the location of copper in the $M(1)O_6$ sites.

TABLE 6
Nature and Number of the Cations Occupying the Different Sites in the Compounds Related to α-$Cu_{4.05}Cr_{3.3}(VO_4)_6$ and α-$Cu_4Fe_{3.333}(VO_4)_6$

Compound	$M(1)$	$M(2)$	$M(3)$	Ref.
$Li_3Fe(MoO_4)_3$	Li	0.333 Fe + 0.667 Li	0.333 Fe + 0.667 Li	10
$Li_2Fe_2(MoO_4)_3$[a]	Li	0.5 Li + 0.5 Fe	0.438 Li + 0.562 Fe	10
$Li_{1.60}Mn_{2.20}(MoO_4)_3$	0.434 Mn + 0.566 Li	0.602 Mn + 0.398 Li	0.233 Li + 0.574 Mn + 0.193□	21
$Li_2Zr(MoO_4)_3$[b]	Li	0.5 Li + 0.25 Zr + 0.25 □	0.5 Zr + 0.5□	22
$NaCo_{2.31}(MoO_4)_3$[c]	Na	0.772 Co + 0.228 □	0.766 Co + 0.234□	23
$Cu_{3.85}(MoO_4)_3$[d]	Cu	Cu	0.85 Cu + 0.25□	24
$Li_2Ni_2(MoO_4)_3$	Li	0.731 Ni + 0.269 Li	0.538 Ni + 0.462 Li	25
$Li_2Co_2(MoO_4)_3$	0.21 Co + 0.79 Li	0.66 Co + 0.34 Li	0.51 Co + 0.49 Li	26
$Li_{1.94}Cu_{2.06}(MoO_4)_3$[e]	0.50 Cu + 0.50 Li	0.28 Cu + 0.72 Li 0.49 Cu + 0.51 Li	0.79 Cu + 0.21 Li	27
$Mg_{2.5}VMoO_8$[f]	Mg	Mg	0.9 Mg + 0.1□	28
$Cu_3Fe_4(VO_4)_6$ Lyonsite	Cu	Fe	0.5 Cu + 0.5□[g]	1
$Co_4Fe_{3.33}(VO_4)_6$	Co	0.17 Co + 0.83 Fe	0.662 Co + 0.338□	4
α-$Cu_{4.05}Cr_{3.3}(VO_4)_6$	Cu	0.175 Cu + 0.825 Cr	0.675 Cu + 0.325□	This
α-$Cu_4Fe_{3.333}(VO_4)_6$	Cu	0.167Cu + 0.833 Cr	0.667 Cu + 0.333□	work

[a] The refined composition of the sample was $Li_{2.44}Fe_{1.56}(MoO_4)_3$.
[b] Space group $P2_1mn$.
[c] Authors (10) suggested the following composition for this sample $Na_2Co_2(MoO_4)_3$ and the following cation distributions: Na–$M(1)$, 0.667Co + 0.333Na − $M(2)$, and $M(3)$.
[d] Space group $P2_12_12_1$.
[e] Space group $P2_1/c$.
[f] The given composition changes from the calculated one.
[g] Refined occupancy was 0.59Cu + 0.41□.

eity. The region of homogeneity for double lithium\manganese molybdate $Li_{2-2x}Mn_{2+x}(MoO_4)_3$ was observed for $0 < x < 0.28$ (21). $Li_{3.33}Zr_{0.67}(MoO_4)_3$ and $Li_2Zr(MoO_4)_3$ were found to be isotypic (12, 22). Klevtsova *et al.* (22) supposed the existence of $Li_{2+4x}Zr_{1-x}(MoO_4)_3$ ($0 \le x \le \frac{1}{3}$) solid solution.

Cation distributions over three cation sites in different compounds are given in Table 6. Vacancies are mainly localized in $M(3)O_6$ octahedra. It is likely associated with short distance between the centers of $M(3)O_6$ octahedra that are separated by $a/2$ (2.45 Å for α-$Cu_{4.05}Cr_{3.3}(VO_4)_6$). Thermal ellipsoids for cations in $M(3)O_6$ octahedra were found to be strongly anisotropic and elongated along the a axis (1, 21–23). It may indicate a slight displacement of cations in $M(3)O_6$ octahedra towards the vacant $M(3)O_6$. This displacement may reduce the repulsion of cations in $M(3)O_6$ octahedra (1, 21). Alkali and Me^{2+} (Me = Co and Mn) cations in $M(1)O_6$ trigonal prisms are located in the center of these prisms (4, 9, 21–23, 25–27), while copper cations in lyonsite (1), α-$Cu_4Fe_{3.333}(VO_4)_6$, and α-$Cu_{4.05}Cr_{3.3}(VO_4)_6$ (Fig. 7d) lie on the prism face and actually have a square-planar coordination, typical for Cu^{2+}.

ACKNOWLEDGMENTS

This work was supported by the Russian Foundation for Basic Research Grant 00-03-32660.

REFERENCES

1. J. M. Hughes, S. J. Starkey, M. L. Malinconico, and L. L. Malinconico, *Am. Mineral.* **72,** 1000 (1987).
2. M. A. Lafontaine, J. M. Greneche, Y. Laligant, and G. Ferey, *J. Solid State Chem.* **108,** 1–10 (1994), doi:10.1006/jssc.1994.1001.
3. L. Permer, Y. Laligant, G. Ferey, and Y. Calage, *J. Solid State Chem.* **107,** 539–546 (1993), doi:10.1006/jssc.1993.1379.
4. X. Wang, D. A. Vander Griend, C. L. Stern, and K. R. Poeppelmeier, *Inorg. Chem.* **39,** 136 (2000).
5. J. M. Hughes, J. W. Drexler, C. F. Campana, and M. L. Malinconico, *Am. Mineral.* **73,** 181 (1988).
6. A. A. Belik, *Mater. Res. Bull.* **34,** 1973 (1999).
7. A. A. Belik, A. P. Malakho, K. V. Pokholok, B. I. Lazoryak, and S. S. Khasanov, *J. Solid State Chem.* **150,** 159–166 (2000), doi:10.1006/jssc.1999.8572.
8. C. Gicquel-Mayer, M. Mayer, and G. Perez, *Acta Crystallogr. B* **37,** 1035 (1981).
9. R. F. Klevtsova, V. G. Khim, and P. V. Klevtsov, *Kristallografiya* **25,** 1148 (1980).
10. Yu. A. Gorbunov, B. A. Maksimov, Yu. K. Kabalov, A. N. Ivaschenko, O. K. Melnikov, and N. B. Belov, *Docl. Acad. Nauk SSSR* **254,** 873 (1980).
11. R. F. Klevtsova and S. A. Magarill, *Kristallografiya* **15,** 710 (1970).
12. V. A. Efremov and V. K. Trunov, *Izv. Acad. Nauk. Inorg. Mater.* **11,** 273 (1975).
13. V. A. Efremov and V. K. Trunov, *Zhurn. Neorg. Khim.* **22,** 2034 (1972).
14. A. I. Korosteleva, V. I. Kovalenko, and E. A. Ukshe, *Izv. Acad. Nauk. Inorg. Mater.* **17,** 748 (1981).

15. F. Izumi, *in* "The Rietveld Method" (R. A. Young, Ed.), Chap. 13. Oxford Univ. Press, New York, 1993.
16. B. C. Frazer and P. J. Brown, *Phys. Rev. A* **125,** 1283 (1962).
17. R. E. Newnham and Y. M. De Haan, *Z. Kristallogr.* **117,** 235 (1962).
18. C. Calvo and R. Faggiani, *Acta Crystallogr. B* **31,** 603 (1975).
19. E. Prince, *Acta Crystallogr.* **10,** 554 (1957).
20. F. Menil, *J. Phys. Chem. Solids* **46,** 763 (1985).
21. S. F. Solodovnikov, Z. A. Solodovnikova, R. F. Klevtsova, L. A. Glinskaya, P. V. Klevtsov, and E. S. Zolotova, *Zh. Strukt. Khim.* **35,** 136 (1994).
22. R. F. Klevtsova, A. A. Antonova, and L. A. Glinskaya, *Kristallografiya* **24,** 1043 (1979).
23. J. A. Ibers and G. W. Smith, *Acta Crystallogr.* **17,** 190 (1964).
24. L. Katz, A. Kasenally, and L. Kihlborg, *Acta Crystallogr. B* **27,** 2071 (1971).
25. M. Ozima, S. Sato, and T. Zoltai, *Acta Crystallogr. B* **33,** 2175 (1977).
26. M. Weismann, H. Svoboda, H. Weitzel, and H. Fuess, *Z. Kristallogr.* **210,** 525 (1995).
27. M. Weismann, M. Geselle, H. Weitzel, and H. Fuess, *Z. Kristallogr.* **209,** 615 (1994).
28. V. G. Zubkov, I. A. Leonidov, K. R. Poeppelmeier, and V. L. Kozhevnikov, *J. Solid State Chem.* **111,** 197–201 (1994), doi:10.1006/jssc.1994.1217.